Sites of Covalent Attachment of CYP4 Enzymes to Heme: Evidence for Microheterogeneity of P450 Heme Orientation†

Brian R. Baer,‡ Jason T. Schuman,‡ A. Patricia Campbell,‡ Matthew J. Cheesman,‡ Mariko Nakano,‡ Nicole Moguilevsky,§ Kent L. Kunze,‡ and Allan E. Rettie*,‡

Department of Medicinal Chemistry, University of Washington, Seattle, Washington 98195, and Applied Genetics, Faculty of Science, Universite Libre de Bruxelles, Gosselies, Belgium

Received July 1, 2005; Revised Manuscript Received August 15, 2005

ABSTRACT: Typical cytochrome P450s secure the heme prosthetic group with a cysteine thiolate ligand bound to the iron, electrostatic interactions with the heme propionate carboxylates, and hydrophobic interactions with the heme periphery. In addition to these interactions, CYP4B1 covalently binds heme through a monoester link furnished, in part, by a conserved I-helix acid, Glu310. Chromatography, mass spectrometry, and NMR have now been utilized to identify the site of attachment on the heme. Native CYP4B1 covalently binds heme solely at the C-5 methyl position. Unexpectedly, recombinant CYP4B1 from insect cells and *Escherichia coli* also bound their heme covalently at the C-8 methyl position. Structural heterogeneity may be common among recombinant CYP4 proteins because CYP4A3 exhibited this duality. Attempts to evaluate functional heterogeneity were complicated by the complexity of the system. The phenomenon of covalent heme binding to P450 provides a novel method for assessing microheterogeneity in heme orientation and raises questions about the fidelity of heme incorporation in recombinant systems.

The heme prosthetic group, situated deep within the hydrophobic active site of cytochrome P450 enzymes, serves as the catalytic center for activation of molecular oxygen. Cytochrome P450s employ the activated perferryl species to metabolize a wide range of endogenous and exogenous substrates to both pharmacologically active and inactive products (*1*). In the vast majority of cytochrome P450s characterized to date, the heme is attached to the protein backbone by strictly noncovalent interactions. The most distinguishing interaction is the thiolate coordinate bond between the iron atom and a completely conserved cysteine residue in the C-terminal portion of the protein. Noncovalent interactions between the propionate groups of heme and basic residues of the protein, as well as hydrophobic interactions between the periphery of the heme and the active site pocket, are also important in heme binding to P450s (*2*).

In the past few years, it has become clear that certain members of the CYP4 family, including CYP4B1, also bind their heme group covalently through an ester linkage with a conserved Glu residue in the I-helix of these enzymes and an oxidized heme methyl group (*3*−*7*). A similar phenomenon has been observed in the mammalian peroxidases, including lactoperoxidase, myeloperoxidase, eosinophil peroxidase, and thyroid peroxidase. The crystal structure of myeloperoxidase reveals that the heme is attached to the protein at three locations. Two ester bonds link the C-1 methyl and the C-5 methyl group to the carboxyl groups of Glu242 and Asp94, respectively. In addition, a thioether sulfonium bond is observed between the β-carbon of the 2-vinyl group and Met243 (*8*). The prosthetic heme group released from lactoperoxidase upon digestion has been identified by NMR[1] and mass spectrometric methods as the 1,5-dihydroxymethyl derivative of heme, implying that two ester bonds link the heme to the protein (*9*, *10*). Sequence alignments and mutagenesis studies indicate further that Asp255 is bound to the heme C-5 methyl and Glu375 is bound to the heme C-1 methyl of lactoperoxidase (*11*).

Recently, it was concluded that certain rat CYP4A and 4F forms covalently bound their heme at the C-5 methyl position, based on a chromatographic comparison of hydroxymethylhemes released from recombinant forms of the P450s and lactoperoxidase (*5*, *6*). The identities of lactoperoxidase-derived 1- and 5-hydroxymethylhemes were inferred from studies conducted with active site mutants that sequentially disrupted the enzyme's 1,5-diester heme link (*11*), but no detailed structural analyses in support of these assignments are available. Therefore, the aim of the present study was to unambiguously determine the complementary site of attachment on the heme prosthetic group of rabbit CYP4B1 using chromatography, mass spectrometry, and NMR. Unexpectedly, we found evidence for microheterogeneity in heme orientation in the recombinant but not the native proteins. Potential reasons for this difference and possible implications are discussed.

† This investigation was supported by NIH Grants GM49054 and GM07750.

* To whom correspondence should be addressed. Telephone: (206) 685-0615. Fax: (206) 685-3252. E-mail: rettie@u.washington.edu.

‡ University of Washington.

§ Universite Libre de Bruxelles.

[1] Abbreviations: NMR, nuclear magnetic resonance spectroscopy; HRP, horseradish peroxidase; rLPO, recombinant lactoperoxidase; HPLC, high-performance liquid chromatography; ROESY, rotating frame Overhauser spectroscopy; LC/ESI-MS, liquid chromatography/electrospray ionization mass spectrometry; GC/MS, gas chromatography/mass spectrometry; BSTFA, *N*,*O*-bis(trimethylsilyl)trifluoroacetamide; IPO, 4-ipomeanol.

10.1021/bi051267j CCC: $30.25
Published on Web 09/29/2005

MATERIALS AND METHODS

Enzymes. CYP4B1 was purified from rabbit lung microsomes, *Escherichia coli* (DH5αF′IQ) cell paste, or insect cells (*Trichoplusia ni* H5B1-4) (*12*−*14*). CYP4A3 was expressed in *E. coli* essentially as previously described (*6*). Recombinant enzyme preparations were harvested at 48 h. Horseradish peroxidase (HRP) was purchased from Sigma. Recombinant lactoperoxidase (rLPO) was expressed in CHO cells and purified as reported previously (*15*).

Heme Standards. An authentic standard of 8-hydroxymethylheme was prepared from phenyldiazene-treated HRP according to published procedures (*16*). Lactoperoxidase was used as source of 1-hydroxymethylheme and 5-hydroxymethylheme, based on a report that recombinant forms of lactoperoxidase contain small amounts of these intermediates (*10*, *17*).

Heme Extraction. CYP4B1, CYP4A3, or rLPO was treated with 1 M NaOH for 15 min to hydrolyze the ester linkage, followed by addition of an equal volume of 16 M urea. HRP did not require treatment prior to extraction. Solutions were acidified with TFA before extracting the heme with a 2× volume of ether. The ether was washed with a 1× volume of distilled water, then with a 1× volume of a saturated NaCl solution. Extracts were evaporated to approximately 200 μL, at which point 200 μL of methanol was added. The volume was again reduced to 200 μL, removing the majority of the ether.

Chromatography. The samples were loaded onto a 4.6 mm × 250 mm analytical 5 μm C-4 column (Vydac, Hesperia, CA) for separation. HPLC analysis was performed on a Shimadzu instrument consisting of two LC-10ADvp pumps, an SPD-M10Avp UV−Vis detector, an SCL-10Avp controller, and an SIL-10ADvp autosampler (Shimadzu Scientific Instruments, Inc., Columbia, MD). During analysis, data were collected using EZSTART chromatography software (v 7.2, Shimadzu Scientific Instruments, Inc.) running on Windows 2000. Initial conditions were 55% Solution A (0.05% TFA in H_2O) and 45% Solution B (0.05% TFA in acetonitrile) at a flow rate of 1 mL/min. The linear gradient increased B from 45 to 55% between 0 and 60 min. Heme elution was monitored by absorption at a wavelength of 400 nm. Under these conditions, dihydroxymethylheme eluted at 11 min, 1-hydroxymethylheme at 23.4 min, 5-hydroxymethylheme at 28.9 min, 8-hydroxymethylheme at 30.7 min, and free heme at 44.7 min.

LC/MS Conditions. LC/ESI-MS analysis was performed using a Micromass Quattro II tandem quadrupole mass spectrometer (Micromass, Ltd., Manchester, U.K.) coupled to a Shimadzu LC instrument similar to that described above. The mass spectrometer was run in electrospray ionization (ESI) mode at a cone voltage of 40 V, source block temperature of 180 °C, and a desolvation temperature of 350 °C. Data analysis was carried out using Windows NT-based Micromass MassLynxNT 3.2 software. The total flow into the mass spectrometer was 350 μL/min. The isotopic masses for dihydroxymethylheme (*m*/*z* 646−653) were monitored from 5 to 20 min, and the isotopic masses for monohydroxymethylheme (*m*/*z* 630−637) were monitored from 20 to 35 min.

Heme Preparation for NMR. Hydroxymethylheme was extracted from approximately 1 μmol of CYP4B1 and loaded onto a 10 mm × 250 mm semipreparative 5 μm C-4 column (Vydac, Hesperia, CA). The Shimadzu HPLC instrument described above was used for purification. Initial conditions were 65% Solution A (0.05% TFA in H_2O) and 35% Solution B (0.05% TFA in acetonitrile) at a flow rate of 3 mL/min. The linear gradient increased B from 35 to 45% between 0 and 20 min. Heme elution was monitored by absorption at a wavelength of 400 nm. Under these conditions, hydroxymethylhemes from CYP4B1 eluted at ∼28 min, but 5-hydroxymethylheme and 8-hydroxymethylheme were incompletely resolved on the semipreparative column. Therefore, the leading edge of the earlier eluting, major HPLC peak was collected from approximately 10 injections, lyophilized, and then dissolved in d_5-pyridine. Approximately 5 mg of $SnCl_2$ was added to reduce the heme, and then the sample was transferred to a NMR tube, flushed with argon, and sealed.

NMR Conditions. NMR data were acquired at 500 MHz on a Varian Inova 500 spectrometer equipped with an actively shielded *z*-axis gradient and a triple resonance probe. All experiments were conducted at 25 °C. 1D ^{1}H NMR spectra were acquired with a spectral width of 8000 Hz using 8192 acquired points. The ^{1}H ROESY data set included an 8000 Hz spectral width, 320 transients, 128 increments, and 8192 points along F_2. ROESY experiments were acquired with a mixing time of 300 ms. 2D data sets were processed using MestRe-C software (version 3.5.9, http://www.mestrec.com).

Lauric Acid Hydroxylation Activity. Rabbit CYP4B1 (10 pmol of each purified form) was preincubated with P450 reductase (40 pmol), cytochrome b_5 (10 pmol), catalase, (100 units), and 20 μg of L-α-dilauroylphosphatidylcholine (DLPC). Metabolic reactions were carried out in 0.1 M potassium phosphate buffer, pH 7.4, containing 1−100 μM lauric acid and 0.5 mM NADPH at 37 °C. The total volume of the reconstituted mixture was 2 mL. Reactions were terminated after 10 min by the addition of 1 mL of 10% HCl and spiked with internal standard, 15-hydroxypentadecanoic acid (2 nmol). The metabolites were extracted with 3 mL of ethyl acetate, dried under nitrogen, and derivatized with BSTFA. Metabolites generated from the incubation of CYP4B1 and lauric acid were quantified using a Shimadzu GC/MS (Shimadzu Scientific Instruments, Inc., Columbia, MD). The gas chromatograph (GC-17A) was equipped with a 30 m × 250 μm capillary XTI-5 column (Restek Corp., Bellefonte, PA). The carrier gas was helium with a constant flow rate of 1 mL/min. The injection port temperature was 250 °C. The temperature gradient was increased from 120 to 160 °C at a rate of 20°/min, then from 160 to 210 °C at a rate of 4°/min, and finally from 210 to 280 °C and held at 280 °C for 2 min. The column was connected to a Shimadzu mass spectrometer (GCMS-QP5050). The interface temperature was 300 °C, and the detector voltage was 1.6 V throughout the method. The following metabolites were observed and confirmed with standards: 10-hydroxy lauric acid (11.5 min, *m*/*z* 131), 11-hydroxy lauric acid (11.8 min, *m*/*z* 117), and 12-hydroxy lauric acid (13.2 min, *m*/*z* 345). 15-Hydroxypentadecanoic (17.1 min, *m*/*z* 387) was used as an internal standard. Ions were monitored in selected-ion monitoring mode with an interval time of 50 ms. Data were analyzed on using GC/MSsolution version 1.10 beta software (Shimadzu Scientific Instruments, Inc., Columbia, MD).

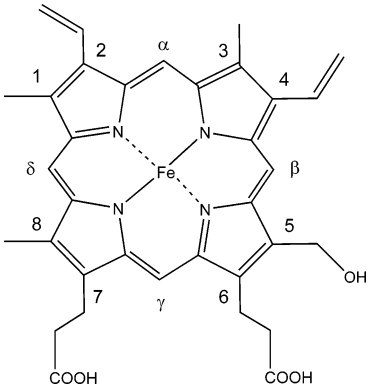

FIGURE 1: Structure of 5-hydroxymethylheme.

4-Ipomeanol (IPO) Bioactivation Activity. Purified P450 (200 pmol) was reconstituted with P450 reductase (400 pmol), DLPC (20 μg), and cytochrome b_5 (200 pmol) in 100 mM potassium phosphate buffer (pH 7.4). *N*-Acetyl cysteine and *N*-acetyl lysine were then introduced in 100 mM potassium phosphate buffer to a final concentration of 10 mM each to trap the reactive enedial intermediate (*18*). IPO was then added to a final concentration of 1 mM (using a 10 mM stock solution made in 10% methanol). The total volume of the reconstituted mixture was 0.5 mL. Metabolic activity was initiated by the addition of NADPH (1 mM final concentration), and incubations were allowed to proceed at 37 °C for 30 min. Reactions were terminated by the addition of 50 μL of a 15% zinc sulfate. The rates of bioactivation of IPO were determined by HPLC analysis of a stable pyrrole adduct as previously described (*18*).

RESULTS

Chromatographic Separation of Monohydroxymethylhemes. Recombinant LPO-derived 1- and 5-hydroxymethylhemes (Figure 1) and HRP-derived 8-hydroxymethylheme were well-separated on a Vydac C4 HPLC column (Figure 2A,B). The monohydroxymethylheme released from native rabbit lung CYP4B1 eluted at the same retention time (28.9 min, Figure 2C) as the minor and later eluting isomer generated from incompletely processed rLPO, and so was tentatively identified as 5-hydroxymethylheme (*11*).

NMR Analysis of 5-Hydroxymethylheme. To unambiguously establish the site of covalent attachment of native CYP4B1 to its heme, ~25 mg of purified recombinant enzyme was prepared and monohydroxymethylheme was released by base hydrolysis for structural elucidation by NMR. The heme that coeluted with the 5-hydroxymethylheme biosynthetic standard was collected, lyophilized, dissolved in d_5-pyridine, and treated with tin chloride. A ROESY 2D NMR spectrum of this sample is shown in Figure 3. The location of the hydroxyl group of this monohydroxymethylheme was identified by the chemical shift changes compared to unmodified heme (Table 1). The most valuable ROE signal used to definitively assign the structure is the cross-peak between the *β-meso* proton (10.59 ppm) and the 5-hydroxymethylene protons (6.31 ppm). The signal for the methylene protons, to which the hydroxyl group is attached, is shifted 2.83 ppm downfield when compared to the 5-methyl protons in heme (3.48 ppm). The signal for the *β-meso* proton is 0.46 ppm downfield compared to the *β-meso* proton in heme (10.13 ppm). Although we did not have sufficient quantities of heme from recombinant lactoperoxidase for NMR analysis, we did obtain 1D and 2D ROESY spectra of the 8-hydroxymethylheme generated from horseradish peroxidase (*16*). The chemical shift alterations due to the hydroxyl group at the 5-methyl position agree well with the corresponding chemical shift changes observed

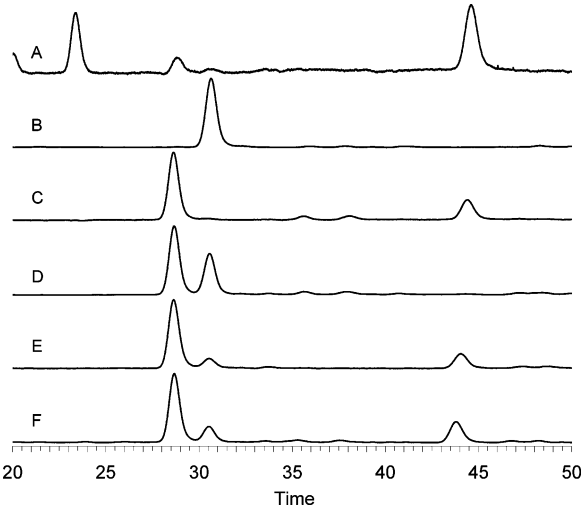

FIGURE 2: Chromatographic analysis of monohydroxymethylhemes. Modified hemes were monitored by absorbance at 400 nm: (trace A) 1-hydroxymethylheme (23.4 min) and 5-hydroxymethylheme (28.9 min) hydrolyzed from rLPO and free heme (44.7 min); (trace B) 8-hydroxymethylheme (30.7 min) from phenylhydrazine-treated HRP; (trace C) hemes released by hydrolyzing the ester linkage in native CYP4B1; (trace D) hemes released by hydrolyzing the ester linkage in recombinant CYP4B1, expressed in insect cells; (trace E) hemes released by hydrolyzing the ester linkage in recombinant CYP4B1, expressed in *E. coli*; (trace F) hemes released by hydrolyzing the ester linkage in recombinant CYP4A3.

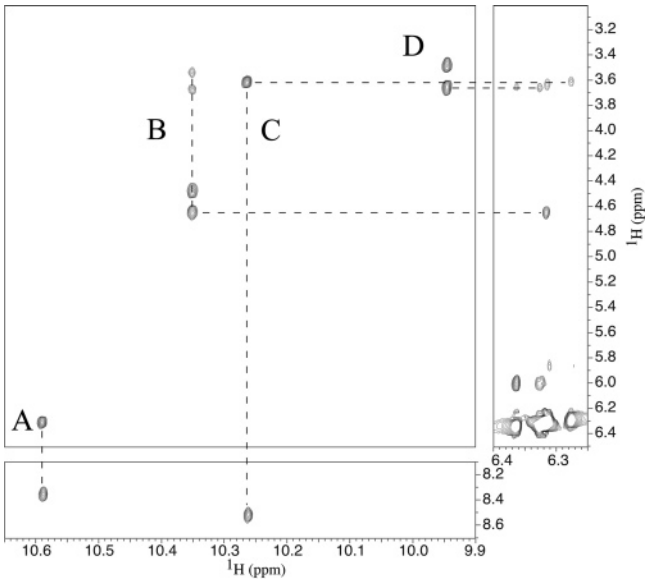

FIGURE 3: 2D NMR ROESY spectrum for the bis-pyridine complex of ferrous 5-hydroxymethylheme in d_5-pyridine. (A) The *β-meso* proton connectivity with 5-methylene and 4α-vinyl protons. (B) The *γ-meso* proton connectivity with 7*β*, 6*β*, 7α, and 6α propionic protons; the 6α-propionic protons also show a connectivity with the 5-methylene protons. (C) The α-*meso* proton connectivity with 3-methyl and 2α-vinyl protons; the 3-methyl protons also show a connectivity with the *trans*-4*β*-vinyl protons. (D) The *δ-meso* proton connectivity with 8-methyl and 1-methyl protons; the 1-methyl protons also show a connectivity with the *trans*-2*β*-vinyl protons.

Table 1: Chemical Shifts for Protons in Heme, HRP-Derived 8-Hydroxymethyl Heme (8-OH), CYP4B1-Derived 5-Hydroxymethyl Heme (5-OH), and Observed ROE Interactions

	chemical shift (δ, ppm)			
proton	heme	8-OH	5-OH	ROE interaction
α-*meso*	10.30	10.26	10.26	3-methyl, 2α-vinyl
β-meso	10.13	10.14	10.59	5-methyl (methylene), 4α-vinyl
δ-meso	9.96	10.43	9.95	1-methyl, 8-methyl (methylene)
γ-meso	10.35	10.42	10.35	6α, 6*β*, 7α, and 7*β*-propionic
1-methyl	3.67	3.54	3.65	*δ-meso*, 2*β*-vinyl (trans)
3-methyl	3.65	3.65	3.61	α-*meso*, 4*β*-vinyl (trans)
5-methyl(ene)	3.48	3.49	6.31	*β-meso*, 6α-propionic
8-methyl(ene)	3.51	6.37	3.48	*δ-meso*, 7α-propionic
2α-vinyl	8.54	8.49	8.52	2*β*-vinyl (cis),2*β*-vinyl (trans),α-*meso*
4α-vinyl	8.48	8.51	8.35	4*β*-vinyl (cis), 4*β*-vinyl (trans), *β-meso*
2*β*-vinyl (trans)	6.34	6.30	6.35	2α-vinyl, 1-methyl, 2*β*-vinyl (cis)
4*β*-vinyl (trans)	6.32	6.32	6.29	4α-vinyl, 3-methyl, 4*β*-vinyl (cis)
2*β*-vinyl (cis)	5.98	6.01	6.00	2α-vinyl, 2*β*-vinyl (trans)
4*β*-vinyl (cis)	6.00	5.96	5.86	4α-vinyl, 4*β*-vinyl (trans)
6α-propionic	4.52	4.52	4.64	6*β*-propionic, *γ-meso*, 5-methyl(ene)
7α-propionic	4.52	4.71	4.48	7*β*-propionic, *γ-meso*, 8-methyl(ene)
6*β*-propionic	3.56	3.57	3.67	6α-propionic, *γ-meso*
7*β*-propionic	3.56	3.72	3.54	7α-propionic, *γ-meso*

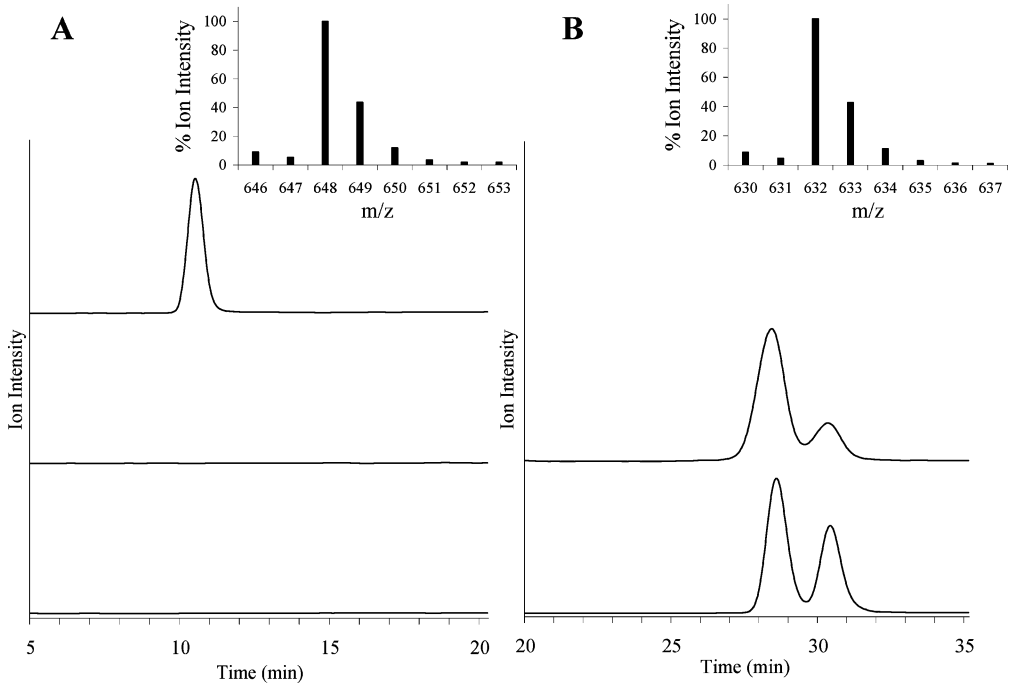

FIGURE 4: Selected ion monitoring chromatograms for CYP4B1, CYP4A3, and LPO. (A) The mass for dihydroxymethylheme (*m*/*z* 648) was monitored from 5 to 20 min for CYP4B1 (lower trace) and CYP4A3 (middle trace). The SIR trace for 1-,5-dihydroxymethylheme from LPO (upper trace) is included as a positive control. (B) The mass for monohydroxymethylheme (*m*/*z* 632) was monitored from 20 to 35 min for CYP4B1 (lower trace) and CYP4A3 (upper trace). The relative ion intensities for the isotopic masses of each heme are shown in the inset.

due to the hydroxyl group at the 8-methyl position (Table 1).

Microheterogeneity of Heme Incorporation into Recombinant CYP4 Enzymes. Unlike the native enzyme, recombinant CYP4B1 expressed in insect cells or *E. coli* contained a mixture of hemes (Figure 2D,E). The major heme species was 5-hydroxymethylheme, as observed in the native form of the enzyme. The minor peak—13% of the total monohydroxymethylheme in CYP4B1 expressed in insect cells and 40% of the total monohydroxymethylheme in CYP4B1 expressed in *E. coli*—coeluted with the 8-hydroxymethylheme standard. CYP4A3 expressed in *E. coli* exhibited a similar heme profile, with the majority of heme aligning with the 5-hydroxymethylheme peak and 20% of the heme coeluting with 8-hydroxymethylheme (Figure 2F).

Alternative Origins of 8-Hydroxymethylheme. To evaluate the possibility that 8-hydroxymethylheme present in recombinant CYP4 preparations derived from the incomplete processing of a 5,8-diester link, we performed selected-ion monitoring at *m*/*z* 648 using lactoperoxidase as a positive control. No evidence was found for any dihydroxymethylheme species from either CYP4B1 or CYP4A3 (Figure 4A). Figure 4B shows that the *m*/*z* 632 traces for both CYP4B1 and CYP4A3 agree with the 400 nm absorption traces in Figure 2. The isotopic patterns for both species match with predicted values (Figure 4B, inset). Another possibility to

Table 2: Heterogeneity of Covalent Heme Binding and Functional Characteristics of Native and Recombinant CYP4B1[a]

	% bound heme			LA hydroxylation			
expression system	5-methyl	8-methyl	% free heme	V_{max}	K_m	ω/ω-1	IPO-bioactivation
rabbit lung	80		20	24.5 ± 2.6	37 ± 10	1.3	683 ± 43
	100	0					
insect cells	81		19	13.7 ± 0.7	26 ± 3	1.5	715 ± 52
	87	13					
E. coli	100		0	14.6 ± 1.4	35 ± 8	1.4	560 ± 38
	62	38					

[a] The V_{max} for lauric acid (LA) hydroxylation represents the rate for ω-hydroxylation and is expressed as (nmol/nmol P450)/min, and the K_m is expressed as μM. The rate for 4-ipomeanol (IPO) bioactivation is expressed as (nmol/nmol P450)/30min.

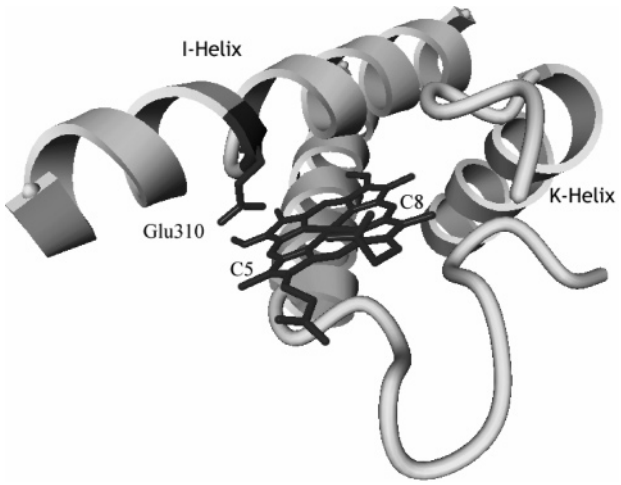

FIGURE 5: CYP4B1 homology model structured after $P450_{BM3}$. The heme is shown flanked by the L-helix and the I-helix, which contains Glu310. The protein backbone extending from the L- and K-helices is in close proximity to the C8 methyl group, but lacks any aspartate or glutamate residues.

consider is that that the minor 8-hydroxymethylheme isomer originated from an ester linkage to an amino acid other than Glu310. To probe this further, we inspected a homology model of rabbit CYP4B1, structured after another fatty acid hydroxylase, $P450_{BM3}$. The homology model reveals a single glutamate near the heme periphery (Figure 5). The carboxylate group of Glu310 on the I-helix, previously identified as the site of protein attachment, is located just 3.3 Å from the C-5 methyl group of the heme. There are no glutamate or aspartate residues within close proximity to the C-8 methyl group, which could potentially form a second ester linkage.

Functional Comparisons of CYP4B1 Activity. Lauric acid was hydroxylated at the ω-position by native and recombinant forms of CYP4B1 at maximal rates of 14−25 (nmol/nmol)/min and with similar K_m values of 26−37 μM (Table 2). The ω/ω-1 regioselectivity was ~1.4 for these three CYP4B1 preparations. Likewise, IPO was bioactivated by native CYP4B1 and both recombinant forms at near equivalent rates of 560−715 (nmol/nmol)/30min (Table 2). These data are not indicative of gross differences in functional activity between the structurally heterogeneous forms of CYP4B1.

DISCUSSION

The covalently attached prosthetic group in CYP4B1 presents a unique opportunity to examine the orientation of the heme relative to the P450 protein structure. After hydrolyzing the ester linkage between the heme and Glu310 of CYP4B1, the resulting hydroxymethylheme isomer retains information about the original position in relation to the I-helix. Chromatography and NMR analysis of heme released upon mild base hydrolysis of native rabbit lung CYP4B1 revealed that the heme species is exclusively the 5-hydroxymethylheme isomer, which places the C-ring of the heme in close proximity to the I-helix. Surprisingly, recombinant preparations of CYP4B1 yielded a second monohydroxymethylheme that co-chromatographed with authentic 8-hydroxymethylheme. Mass spectrometry data argued against a di-ester linkage to CYP4B1, and homology modeling of the active site of rabbit CYP4B1 provided no support for an alternative amino acid partner. Collectively, these observations suggest that heme is inserted into recombinant CYP4B1 in two distinct orientations that are related by a 180° rotation about the heme α−γ-*meso* carbon axis.

The current studies also suggest that differential heme insertion is a general phenomenon, at least in recombinant CYP4 enzymes, because *E. coli*-expressed CYP4B1 and CYP4A3 both contained a mixture of the modified hemes following ester hydrolysis. Previous chromatographic analysis of recombinant CYP4A8, CYP4A3/E318D, and CYP4F5/G330E hemes, suggested covalent attachment at only the C-5 position (*5*, *6*). In these earlier studies, the extent of covalent heme attachment was generally lower than reported here, and so expression conditions may be an important variable.

Conformationally distinct (A and B) orientations of heme in cytochrome b_5 have been known for 25 years (*19*). The ratio of the resulting conformers is a function of steric restraints imposed by amino acid side chains lining the heme cavity, which helps rationalize the vastly differing A/B ratios evident in cytochrome b_5 from different species (*20*). Much of this information is derived from NMR studies of the protein, as crystal structures have not generally been of sufficient resolution to discriminate between the two isomers (*21*). However, recent high-resolution X-ray crystallography studies of *Mycobacterium tuberculosis* CYP121, expressed in *E. coli*, are indicative of a 70:30 mixture of the two heme orientations posited here for CYP4B1 and CYP4A3 (*22*). In addition, the structure of CYP154A1 from *Streptomyces coelicolor* A3(2), also expressed in *E. coli*, has revealed that the heme is present in a 180°-flipped orientation (*23*). While good evidence exists for different heme conformers in cytochrome b_5 and bacterial P450s, the present studies provide the first evidence for multiple heme conformers in mammalian P450.

An alternative method for evaluating P450 heme stereochemistry has been developed that takes advantage of the alkylated heme adducts formed from 3,5-bis(carbethoxy)-2,6-dimethyl-4-ethyl-1,4-dihydropyridine (DDEP) during catalytic turnover (*24*). This method allows the analysis of heme orientation in mammalian P450s, for which no sufficiently high-resolution structures yet exist to discriminate between heme conformers. Circular dichroism spectra of the C-ring isomer of the *N*-ethylprotoporphyrin IX hemes formed from native rat P450 revealed optical purity similar to that of hemoglobin, in which the heme is known to be in a single orientation (*24*). This result agrees with the single hydroxymethylheme stereoisomer that was found in native CYP4B1 purified from rabbit lung. On the basis of these findings, multiple heme orientations may not be important for P450s expressed in their native environment but could be a general phenomenon for recombinant P450 enzymes.

The presence of an ester linkage to the 8-methyl group of heme in the recombinant forms of CYP4B1 indicates that the fidelity of the heme insertion process and/or the protein folding process that occurs in the rabbit lung is not replicated in the bacterial or insect cell expression systems. Bacterial P450s and cytochrome b_5 permit the facile exchange of heme ligands without denaturating the enzyme, in contrast to eukaryotic P450s where the heme insertion process during folding could well be very different. One plausible explanation for the altered heme orientations from native and recombinant mammalian P450 is that protein folding chaperones in the various expression systems (rabbit lung, insect cells, and *E. coli*) are not identical. There is little information in the literature available to date about P450 heme−protein assembly, but there is evidence for the involvement of chaperones in the process. In phenobarbital-pretreated rats, Zgoda et al. discovered a possible role for the chaperone GRP94 in heme−protein assembly (*25*). GRP94 is shown to assist in restoring allylisopropylacetamide-inactivated CYP2B1 by exchanging the N-alkylated heme for unmodified heme and is described as a "finishing" chaperone in the biosynthesis and/or assembly of ER proteins (*25*). Inoue et al. found that holo-CYP3A7 could only be expressed in *E. coli*. when the molecular chaperone GroEL was coexpressed, indicating that the bacteria did not contain the appropriate protein folding/heme insertion machinery for production of the mammalian P450 (*26*). Therefore, it is possible that heme insertion is facilitated by distinct chaperones in *E. coli*, which do not have the same stringency for stereoselective incorporation of heme as the mammalian forms. Inefficient heme insertion by insect cell chaperones might also offer an explanation for why recombinant human CYP4B1 holoenzyme is not expressed successfully using the baculovirus expression vector system (*14*). Possibly, with the appropriate chaperone machinery in mammalian tissues, heme can be correctly incorporated into human CYP4B1 to produce active protein (*27*).

Microheterogeneity of heme orientation in recombinant P450 enzymes raises the possibility of multiple heme−protein species with altered catalytic activity, because steric interactions between the heme-binding cavity in the protein and the repositioned vinyl and methyl groups of the heme may influence active site conformation. This could have important ramifications for the industrial drug discovery process where recombinant P450 enzymes are used routinely to evaluate and make predictions about in vivo drug metabolism (*28*). Therefore, we examined lauric acid metabolism and 4-ipomeanol bioactivation rates to evaluate the effect of heme orientation in CYP4B1 on substrate turnover. With lauric acid, the regioselectivity of ω/ω-1 hydroxylation of lauric acid was similar for all enzymes, suggesting that the active site conformation is unaffected. Apparent K_m and V_{max} values for laurate varied by less than 2-fold, and IPO bioactivation rates were similar across the three enzyme preparations. No definitive trends could be observed, and so these studies do not provide evidence for modified monooxygenase activity due to altered heme orientation in CYP4B1. However, the activity contribution of CYP4B1 with heme bound to the 8-methyl position is difficult to assess because of intrinsic variability in enzyme activities from purified P450 preparations and a lack of knowledge concerning the orientation of the heme component that is not covalently bound. Moreover, electron transfer and oxygen binding could potentially be affected by a reoriented heme. An altered redox potential has been reported for the two heme conformers of cytochrome b_5, but the magnitude of the change is believed to be too small to be functionally significant (*29*). Additional studies are required to deconvolute this complex system in cytochrome P450 in order to more definitively address the question of functional heterogeneity secondary to promiscuous heme processing by recombinant CYP4 proteins.

In conclusion, chromatography and 2D NMR experiments establish that the structure of the major heme species released from CYP4B1 upon base treatment is 5-hydroxymethylheme. Covalent binding of heme to the C-8 methyl group also occurs to a minor extent with recombinant CYP4 proteins, suggesting that the fidelity of holoenzyme assembly for mammalian P450s is not necessarily recapitulated in heterologous expression systems. The phenomenon of covalent heme binding to CYP4 proteins provides a novel method for assessing microheterogeneity in heme orientation to the mammalian P450s in the absence of high-resolution crystallographic data or solution structures.

ACKNOWLEDGMENT

The rabbit CYP4B1 homology model was generated in the laboratory of Dr. Jeffrey P. Jones at the Department of Chemistry, Washington State University.

REFERENCES

1. Guengerich, F. P. (2001) Common and uncommon cytochrome P450 reactions related to metabolism and chemical toxicity, *Chem. Res. Toxicol. 14*, 611−650.
2. Williams, P. A., Cosme, J., Ward, A., Angove, H. C., Matak Vinkovic, D., and Jhoti, H. (2003) Crystal structure of human cytochrome P450 2C9 with bound warfarin, *Nature 424*, 464−468.
3. Hoch, U., and Ortiz De Montellano, P. R. (2001) Covalently linked heme in cytochrome P4504A fatty acid hydroxylases, *J. Biol. Chem. 276*, 11339−11346.
4. Henne, K. R., Kunze, K. L., Zheng, Y. M., Christmas, P., Soberman, R. J., and Rettie, A. E. (2001) Covalent linkage of prosthetic heme to CYP4 family P450 enzymes, *Biochemistry 40*, 12925−12931.
5. Lebrun, L. A., Xu, F., Kroetz, D. L., and Ortiz De Montellano, P. R. (2002) Covalent attachment of the heme prosthetic group in the CYP4F cytochrome P450 family, *Biochemistry 41*, 5931−5937.

6. Lebrun, L. A., Hoch, U., and Ortiz De Montellano, P. R. (2002) Autocatalytic mechanism and consequences of covalent heme attachment in the cytochrome P4504A family, *J. Biol. Chem. 277*, 12755−12761.
7. Zheng, Y. M., Baer, B. R., Kneller, M. B., Henne, K. R., Kunze, K. L., and Rettie, A. E. (2003) Covalent heme binding to CYP4B1 via Glu310 and a carbocation porphyrin intermediate, *Biochemistry 42*, 4601−4606.
8. Fiedler, T. J., Davey, C. A., and Fenna, R. E. (2000) X-ray crystal structure and characterization of halide-binding sites of human myeloperoxidase at 1.8 Å resolution, *J. Biol. Chem. 275*, 11964−11971.
9. Rae, T. D., and Goff, H. M. (1998) The heme prosthetic group of lactoperoxidase. Structural characteristics of heme l and heme l-peptides, *J. Biol. Chem. 273*, 27968−27977.
10. DePillis, G. D., Ozaki, S., Kuo, J. M., Maltby, D. A., and Ortiz De Montellano, P. R. (1997) Autocatalytic processing of heme by lactoperoxidase produces the native protein-bound prosthetic group, *J. Biol. Chem. 272*, 8857−8860.
11. Colas, C., Kuo, J. M., and Ortiz De Montellano, P. R. (2002) Asp-225 and Glu-375 in autocatalytic attachment of the prosthetic heme group of lactoperoxidase, *J. Biol. Chem. 277*, 7191−7200.
12. Guan, X., Fisher, M. B., Lang, D. H., Zheng, Y. M., Koop, D. R., and Rettie, A. E. (1998) Cytochrome P450-dependent desaturation of lauric acid: isoform selectivity and mechanism of formation of 11-dodecenoic acid, *Chem.-Biol. Interact. 110*, 103−121.
13. Cheesman, M. J., Baer, B. R., Zheng, Y. M., Gillam, E. M., and Rettie, A. E. (2003) Rabbit CYP4B1 engineered for high-level expression in *Escherichia coli*: ligand stabilization and processing of the N-terminus and heme prosthetic group, *Arch. Biochem. Biophys. 416*, 17−24.
14. Zheng, Y. M., Fisher, M. B., Yokotani, N., Fujii-Kuriyama, Y., and Rettie, A. E. (1998) Identification of a meander region proline residue critical for heme binding to cytochrome P450: implications for the catalytic function of human CYP4B1, *Biochemistry 37*, 12847−12851.
15. Watanabe, S., Varsalona, F., Yoo, Y. C., Guillaume, J. P., Bollen, A., Shimazaki, K., and Moguilevsky, N. (1998) Recombinant bovine lactoperoxidase as a tool to study the heme environment in mammalian peroxidases, *FEBS Lett. 441*, 476−479.
16. Ator, M. A., and Ortiz De Montellano, P. R. (1987) Protein control of prosthetic heme reactivity. Reaction of substrates with the heme edge of horseradish peroxidase, *J. Biol. Chem. 262*, 1542−1551.
17. Watanabe, S., Murata, S., Kumura, H., Nakamura, S., Bollen, A., Moguilevsky, N., and Shimazaki, K. (2000) Bovine lactoperoxidase and its recombinant: comparison of structure and some biochemical properties, *Biochem. Biophys. Res. Commun. 274*, 756−761.
18. Baer, B. R., Rettie, A. E., and Henne, K. R. (2005) Bioactivation of 4-ipomeanol by CYP4B1: adduct characterization and evidence for an enedial intermediate, *Chem. Res. Toxicol. 18*, 855−864.
19. Keller, R. M., and Wuthrich, K. (1980) Structural study of the heme crevice in cytochrome b_5 based on individual assignments of the 1H-NMR lines of the heme group and selected amino acid residues, *Biochim. Biophys. Acta 621*, 204−217.
20. Lee, K. B., La Mar, G. N., Kehres, L. A., Fujinari, E. M., Smith, K. M., Pochapsky, T. C., and Sligar, S. G. (1990) 1H NMR study of the influence of hydrophobic contacts on protein-prosthetic group recognition in bovine and rat ferricytochrome b_5, *Biochemistry 29*, 9623−9631.
21. Banci, L., Bertini, I., Rosato, A., and Scacchieri, S. (2000) Solution structure of oxidized microsomal rabbit cytochrome b_5. Factors determining the heterogeneous binding of the heme, *Eur. J. Biochem. 267*, 755−766.
22. Leys, D., Mowat, C. G., Mclean, K. J., Richmond, A., Chapman, S. K., Walkinshaw, M. D., and Munro, A. W. (2003) Atomic structure of *Mycobacterium tuberculosis* CYP121 to 1.06 Å reveals novel features of cytochrome P450, *J. Biol. Chem. 278*, 5141−5147.
23. Podust, L. M., Kim, Y., Arase, M., Neely, B. A., Beck, B. J., Bach, H., Sherman, D. H., Lamb, D. C., Kelly, S. L., and Waterman, M. R. (2003) The 1.92-Å structure of *Streptomyces coelicolor* A3(2) CYP154C1. A new monooxygenase that functionalizes macrolide ring systems, *J. Biol. Chem. 278*, 12214−12221.
24. Ortiz De Montellano, P. R., Kunze, K. L., and Beilan, H. S. (1983) Chiral orientation of prosthetic heme in the cytochrome P-450 active site, *J. Biol. Chem. 258*, 45−47.
25. Zgoda, G. V., Arison, B., Mkrtchian, S., Ingelman-Sundberg, M., and Almira Correia, M. (2002) Hemin-mediated restoration of allylisopropylacetamide-inactivated CYP2B1: a role for glutathione and GRP94 in the heme-protein assembly, *Arch. Biochem. Biophys. 408*, 58−68.
26. Inoue, E., Takahashi, Y., Imai, Y., and Kamataki, T. (2000) Development of bacterial expression system with high yield of CYP3A7, a human fetus-specific form of cytochrome P450, *Biochem. Biophys. Res. Commun. 269*, 623−627.
27. Imaoka, S., Hayashi, K., Hiroi, T., Yabusaki, Y., Kamataki, T., and Funae, Y. (2001) A transgenic mouse expressing human CYP4B1 in the liver, *Biochem. Biophys. Res. Commun. 284*, 757−762.
28. Rodrigues, A. D. (1999) Integrated cytochrome P450 reaction phenotyping: attempting to bridge the gap between cDNA-expressed cytochromes P450 and native human liver microsomes, *Biochem. Pharmacol. 57*, 465−480.
29. Walker, F. A., Emrick, D., Rivera, J. E., Hanquet, B. J., and Buttlaire, D. H. (1988) Effect of heme orientation on the reduction potential of cytochrome b_5, *J. Am. Chem. Soc. 110*, 6234−6240.

BI051267J